

# Angle resolved microwave spectrometer for metamaterial studies

A. F. Starr, P. M. Rye, J. J. Mock, and D. R. Smith<sup>a)</sup>

*Department of Physics, University of California, San Diego, La Jolla, California 92093-0319*

(Received 8 September 2003; accepted 19 January 2004; published 8 March 2004)

We describe an angle resolved microwave spectrometer (ARMS) based on a planar waveguide scattering chamber, capable of acquiring the angular distribution of TE polarized microwaves scattered from samples centered within the chamber. The spacing between the upper and lower conducting circular plates is 0.4 in. ( $\sim 1$  cm), which, with the associated X-band waveguide adapters, fixes the frequency of operation of the ARMS to be optimally within the X-band frequency range (8–12 GHz). Microwave energy can be injected either as an apertured beam via an extended arm connected to the chamber, or via an antenna located in the center of the chamber. Power is detected at a waveguide adapter located on the periphery of the chamber, attached to a rotating arm that has an angular range of  $180^\circ$ . A computer controlled stepper motor attached to the rotating arm facilitates angular scanning with the data acquired at every angle in an automated fashion. The ARMS has excellent reproducibility and signal-to-noise characteristics, making it ideal for characterizing the refraction properties of metamaterial samples, or as a probe of the interaction between antennas and metamaterial substrates. © 2004 American Institute of Physics.

[DOI: 10.1063/1.1669119]

## I. INTRODUCTION

Artificially structured *metamaterials* have become the subject of intense and widespread interest, as they extend the range of properties available from naturally occurring materials and compounds.<sup>1–4</sup> In particular, *electromagnetic* metamaterials have been recently demonstrated for which the effective electric permittivity ( $\epsilon$ ) and the effective magnetic permeability ( $\mu$ ) are simultaneously negative, a property that does not exist in nature.<sup>1</sup> Such metamaterials—often referred to as left-handed, double-negative, or negative index materials—were hypothesized to have unusual and striking electromagnetic properties, including a negative index-of-refraction ( $n$ ).<sup>5</sup> In recent work, left-handed metamaterials have been constructed to operate at microwave frequencies, and the property of negative refractive index confirmed in Snell's law experiments on wedge shaped samples.<sup>6–8</sup> These experiments have demonstrated that new electromagnetic material responses can be realized, and have led to a considerable amount of follow up work and design of metamaterials.

The term metamaterials, as we use it here, refers to artificially structured media based on an array of repeated scattering elements. The dimensions of the scattering elements and their spacing are less than that of the free-space wavelength of the exciting radiation, so that effective medium arguments can be applied to characterize the material by frequency dependent electromagnetic material parameters, such as  $\epsilon$ ,  $\mu$ , and  $n$ . The metamaterials that were used to demonstrate refraction were based on arrays of conducting wires to provide a (negative) electric response,<sup>9,10</sup> and arrays of conducting split ring resonators to provide a (negative) magnetic response.<sup>11</sup> Although the composite metamaterial may appear

very inhomogeneous and complex, it should approximate a continuous material from the electromagnetic standpoint at the frequencies of operation. For the metamaterials thus far demonstrated, the frequencies of operation have typically been in microwave frequency bands.

With the increased focus on new metamaterial properties, there is a need for characterization apparatus to confirm the new properties. In principle, the determination of the electromagnetic properties of a material can be accomplished by a careful measurement of the complex transmission and reflection coefficients.<sup>12</sup> Such measurements are difficult, however, even for continuous materials, and do not specifically probe wave propagation phenomena, such as refraction. While the phenomena associated with metamaterials follow from their material properties, it is useful to test directly those phenomena, in conjunction with other techniques of characterization.

The apparatus we present here was motivated by a need to better quantify the refraction properties of left-handed metamaterials, which are expected to exhibit negative refraction at certain microwave frequencies. However, the apparatus is capable of probing a number of different metamaterial aspects, including the function of a metamaterial used as an antenna backplane. Antenna backplane measurements have become of interest over the past few years in the context of improved antenna efficiency and miniaturization.<sup>13–15</sup>

The design of an angular resolved microwave spectrometer (ARMS) for a Snell's law refraction experiment is conceptually straightforward. The design we present here follows in spirit that utilized in Ref. 6 to confirm the negative refractive index of a wedge-shaped metamaterial sample. The important aspects of a wedge-based refraction experiment are illustrated in Fig. 1. A plane wave is incident normally onto a face of a wedge sample, which is assumed to possess isotropic material properties. If instead the sample

<sup>a)</sup>Electronic mail: drs@sdss.ucsd.edu

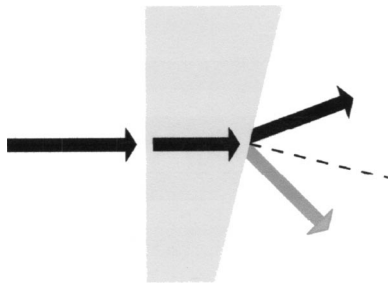


FIG. 1. Depiction of a Snell's law refraction experiment on a wedge sample with isotropic index-of-refraction. The incident electromagnetic wave enters the wedge sample normal to the first interface and refracts at the second interface on either the opposite side (positive refraction) or the same side (negative refraction) of the surface normal as the wave in the medium.

possesses anisotropy, then Fig. 1 still applies so long as the incident propagation direction coincides with a principal axis of the material. After passing through the sample, the wave undergoes refraction at the second interface, which has been cut so as to make an angle with the propagation direction of the incoming wave. For samples with positive refractive index, the exit beam is on the opposite side of the surface normal as the incident beam, as indicated by the black arrow in Fig. 1. For samples with negative refractive index, the exit beam emerges *on the same side of the surface normal as the incident beam*, as indicated by the gray arrow in Fig. 1.

Refraction experiments are easy to perform at visible wavelengths, where well-defined beams that are miniscule in comparison to sample sizes are readily generated. The initial metamaterial samples of interest that have been studied thus far, however, have been designed to operate at microwave frequencies with wavelengths on the order of a few centimeters. This places important design considerations on the measurement apparatus. In particular, as it is costly and difficult to fabricate large metamaterial samples, a primary design goal for the ARMS apparatus is that it facilitate measurements of relatively small metamaterial samples.

The simplest means to minimize the sample volume required is to confine the measurement to two propagation dimensions, leading naturally to the planar waveguide design that has long been used for microwave measurements.<sup>16-18</sup> The lowest mode of a planar waveguide has no cutoff, and is characterized by an electric field polarized uniformly along the direction perpendicular to the plane of the waveguide plates. In the empty chamber, these modes have the identical dispersion characteristics of free space waves. Moreover, because the electric field is always polarized perpendicular to the plane of incidence, as defined by the propagation direction and the normal to any sample surface, the waveguide modes are equivalent to *s*-polarized waves.

In the presence of scattering objects, the equivalence of the waveguide modes to *s*-polarized free-space waves is maintained so long as the materials—or the scattering elements that form the metamaterials—possess reflection symmetry about the center plane between the upper and lower waveguide plates. An implicit assumption made is that the material or metamaterials being studied do not exhibit bianisotropy, which could potentially involve higher order waveguide modes and lead to scattering behavior more dif-

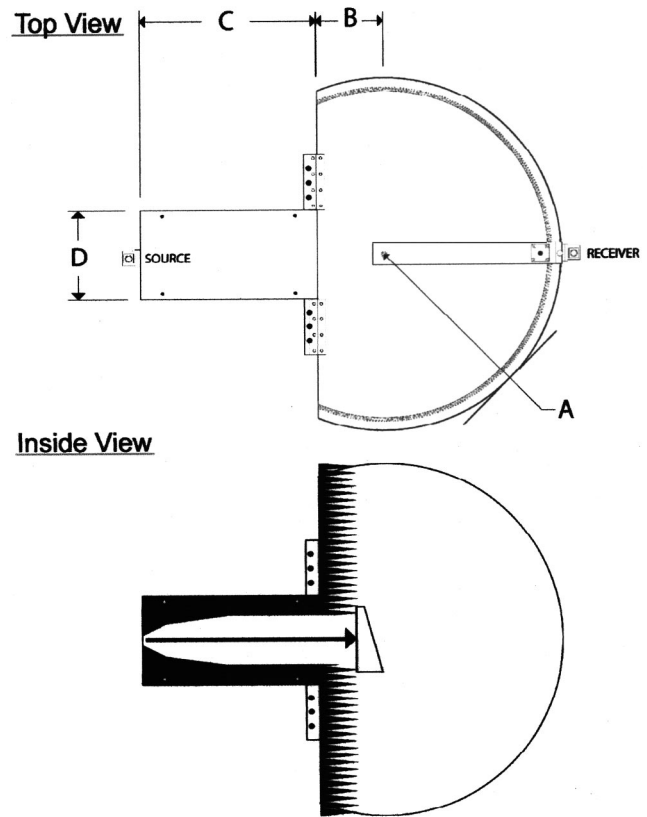


FIG. 2. ARMS apparatus. Planar wave, launched down the rectangular waveguide, interacts with a metamaterial sample placed at the center of the almost semicircular plates ( $A=16$ ,  $B=6$ ,  $C=16$ , and  $D=8$  in., plate spacing = 0.4 in.). The detector, confined to the radius by a bearing mounted arm, sweeps around circumference of the plates driven by the stepper motor. Absorber (in black) is placed inside the plates to minimize unwanted reflective scattering.

ficult to analyze. Bianisotropy and chirality can be mitigated or eliminated by careful metamaterial design.<sup>19</sup> We note also that while the confined geometry allows minimum sample sizes to be considered, the restriction to one polarization—*s* polarization—is a distinct limitation that prevents a full sample characterization. Nevertheless, the advantages offered by the reduced sample size and ease of measurement offset this limitation.

## II. THE ARMS APPARATUS

A diagram of the ARMS apparatus, which bears many features common to the original apparatus that was first developed for negative refraction experiments,<sup>6</sup> is shown in Fig. 2. The design is based on a planar waveguide geometry, with a *central chamber* formed by two semicircular aluminum plates, joined to an *extended channel* formed by two rectangular aluminum plates. The samples generally occupy a small region near the center of the central chamber, and are excited either by a beam launched from the extended channel, or by an antenna that can be inserted into the lower plate of the central chamber.

To approximate the refraction experiment shown in Fig. 1, it is necessary to generate a beam at the sample position that has minimal phase variation perpendicular to the direction of beam propagation, and an apertured beam profile in

the same perpendicular direction that is large compared to the wavelength. Of course the size of the aperture dictates the minimum sample size, therefore it is desirable to limit the aperture size as much as possible. To accomplish this, microwaves are launched from an X-band coax-to-waveguide adapter (HP X281A) mounted on one end of the extended channel. As in the central chamber, the spacing between the bounding conducting (aluminum) plates is 0.4 in. (1.016 cm), with the length of the channel being 16 in. (40.64 cm). The channel in Ref. 6 was 36 in. in length, but this was not deemed to be a critical dimension and was shortened in the present design. Microwave absorber (Microsorb Technologies Inc., MTL-73) lines the sides of the channel, as indicated in Fig. 2, and is used to guide the microwaves from the source to the sample region. The absorber is cut so as to widen the guide region smoothly from the 0.9 in. width of the source waveguide to the 6 in. width of the sample aperture, varying on a scale large compared with the wavelength of the microwaves.

Of particular concern is the possibility of reflection of the scattered waves back into the scattering region, which could produce unwanted artifacts in the data. At all interfaces between the scattering chamber and free space, for example, there exists a substantial impedance mismatch that will reflect some portion of the radiation. A possible means of minimizing or eliminating this reflection would be to line the entire periphery of the chamber with microwave absorber; but this would reduce the signal reaching the external detector, complicate the design and possibly also produce artifacts in the data. A compromise absorber pattern is utilized in the present apparatus, as indicated in Fig. 2 (lower panel), in which a toothed absorber structure is arranged on the back plane of the central chamber. As the subsequent results show, the absence of absorber along the arc of the semicircular plates does not appear to interfere noticeably with the data, e.g., standing wave modes within the chamber are not problematic as the large chamber size and the absorber along the backside sufficiently reduce these unwanted artifacts compared to the expected radiation patterns.

The conclusions drawn from data collected on left-handed metamaterial samples in the initial experiments strongly indicated negative refraction;<sup>6</sup> this conclusion has since been independently confirmed in separate experiments.<sup>7,8</sup> There are, however, many issues that remain to be investigated regarding the nature of negative refraction in metamaterials, requiring the characterization of many different sample configurations. The ARMS apparatus has been developed with the assumption that repetitive measurements will need to be made, with frequent repositioning of samples. Before describing the detailed operation of the present ARMS apparatus, we first note two key improvements over the previous instrument. First, the overall size of the original circular plates set the detector at 6 in. (chamber radius) from the sample surface. Given the aperture used in the experiments—the minimum width of which is dictated by the wavelength—the chamber radius placed the detector within the propagating near-field, or near-Fresnel zone,<sup>20</sup> of the sample. We therefore increased the chamber radius of the ARMS apparatus to 16 in., closer to the far-field limit. The

### Inside View

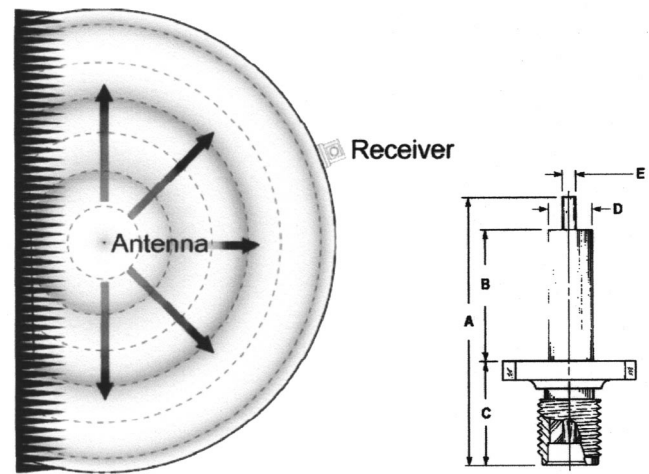


FIG. 3. ARMS apparatus using the optional antenna source ( $A=1.08$ ,  $B=0.315$ ,  $C=0.375$  in., and  $D=0.162$  in. diam,  $E=0.050$  in. diam), combined with experimental backplane sample. Angle resolved radiation pattern is determined by scanning the circumference with the detector.

second improvement was to automate the data acquisition, as the original data were acquired by manually stepping the detector around the circumference of the chamber.

Figure 2 shows the detail and dimensions of the ARMS apparatus. The detector is mounted flush with the chamber on a toothed gear stepper motor, driven by customized software that also controls the data acquisition. The chamber is designed to operate in two modes: in mode 1, the extended channel is used to launch a plane wave onto an aperture that enters the chamber at the center of the circular plates. In mode 2, microwaves are injected into the chamber via a removable coax-fed, source antenna located at the center of the circular plates; mode 2 allows us to make accurate angular resolved measurements of metamaterials used in the context of antenna backplanes (Fig. 3). When using the chamber in mode 2, we extend the backsurface absorber material across the plane wave aperture and insert the antenna through a hole in the bottom plate. Microwaves are generated and detected in the ARMS apparatus by an Agilent vector network analyzer (VNA) model No. 8722. While the frequency range of the VNA is 50 MHz–40 GHz, the plate separation of the planar waveguide restricts our measurements to the frequency band 8–12 GHz, although we find acceptable data can be acquired in the range 8–16 GHz. A data acquisition program, written as a series of macros in Excel visual basic for applications (VBA) controls the stepper motor (Little Step-U TLA Microsystems, Auckland, New Zealand) that rotates the detector arm, in addition to controlling the VNA (Fig. 4).

The VBA language provides enough functionality to handle all aspects of the hardware control, data acquisition, and data manipulation. Access from the computer to the VNA is accomplished via a IEEE-488 interface, while control of the stepper motor driver is through an RS-232 port, using the Microsoft MSCComm32.ocx control. The resulting automation macros precisely coordinate movement and in-

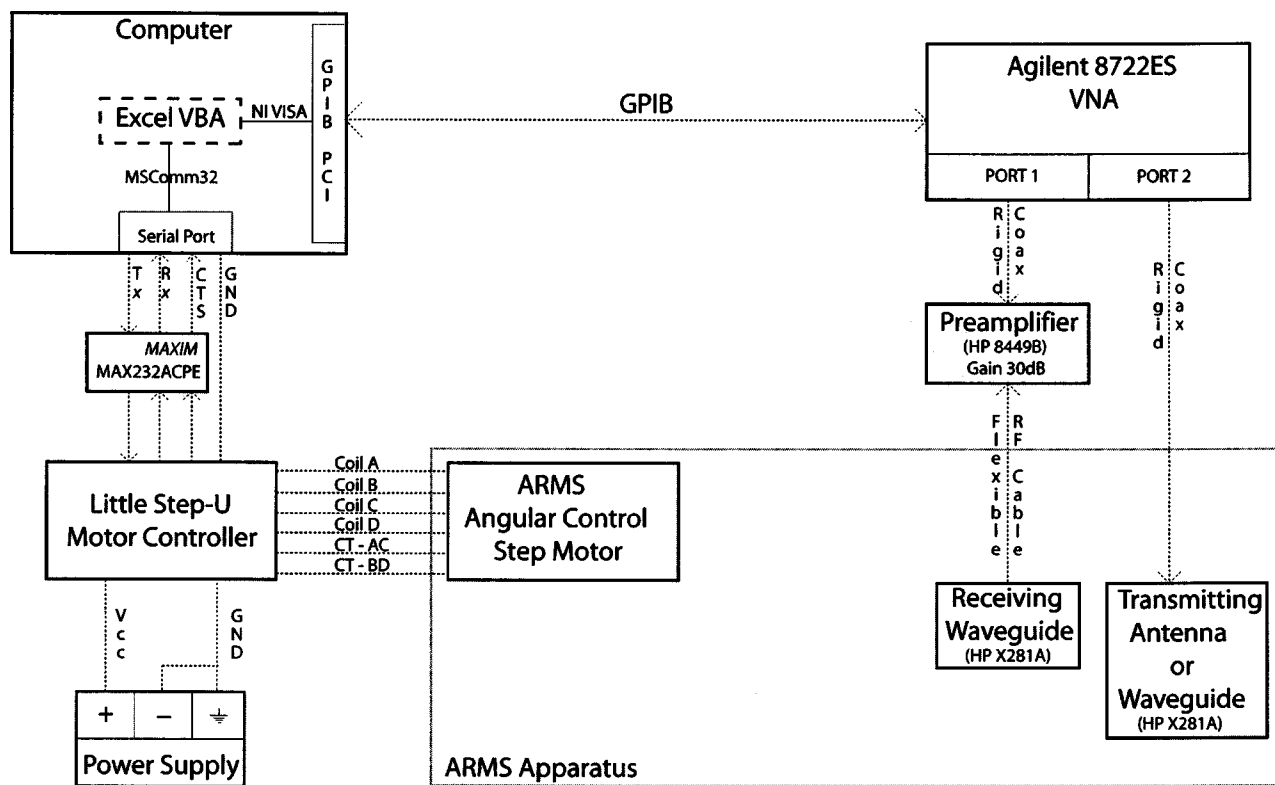


FIG. 4. ARMS apparatus schematic diagram.

strument settings with data acquisition to ensure reproducibility.

The system initialization proceeds with the ARMS control program first reading the state of the VNA, which includes configuration settings such as the start frequency, stop frequency, number of data points, and so forth. The control program energizes the stepper motor windings to lock the detector position at a known starting position. Various angular sweep settings can be set using the control program, including: start and stop angles, angular step size, start and stop frequencies, number of points, and averaging factor. Since the VNA does not output the number of averages performed (only outputs the averaging factor), a waiting function has been included as part of the control program which delays the next angular step until the number of averages equals the averaging factor indicating the conclusion of the averaging function.

The angular stepping motion of the detector induces vibrations in the detector arm. In order to avoid introduction of unwanted structure into the data, a delay (usually 1 s) is used to allow for damping of the vibrations before the control program initiates acquisition or averaging of the data. The maximum number of sampled angles over a specified angular region is currently 256, corresponding to the maximum number of data columns allowed in Microsoft Excel; this limitation, of course, is not inherent to the apparatus and could easily be removed.

To increase our signal to noise ratio, we made use of a preamplifier (HP 8449B). This gives us a gain of about 27.5 dB, a gain flatness of  $\pm 2.5$  dB, and a noise figure of  $-10$  dB over the frequency range of 8–16 GHz. The amplifier causes a loss of symmetry in the  $S$ -parameter measurements, e.g.,

$S_{12} \neq S_{21}$ .  $S_{12}$  and  $S_{22}$  lose meaning since they look into the amplifier output.

The accuracy of the ARMS waveguide apparatus is in part determined by the flatness of the 1/4-in.-thick aluminum plates (rolled sheet aluminum) which make up the upper and lower central chamber plates and the plates of the extended channel. As purchased, the lower central chamber plate was significantly warped. To remedy this, it was necessary to flatten the plate by mounting three 1 in. square aluminum straightening rods to the bottom surface. The rods were drilled with several  $> 1/4$  in. through-holes, with corresponding  $1/4 \times 20$  blind tapped holes machined into the bottom of the lower aluminum plate. When the straightening rods were brought flush with the aluminum plate surface by means of tightening the  $1/4 \times 20$  machine screws, the aluminum plate became nearly flat. Starting with a machine ground 1/4 in. aluminum plate rather than the rolled sheet aluminum might reduce the need for straightening bars.

The inner surfaces of the waveguide plates are required to be free of any protrusions or holes which may present an impedance mismatch to the guided microwaves; any impedance mismatch within the chamber will lead to unwanted scattering, which must be minimized. Threaded mounting holes in the outside of the chamber plates are therefore blind tapped so as not to interfere with the inner surface. The hole in the bottom plate through which the optional source antenna is inserted is covered with aluminum foil that is adhered flat using a spray-on glue when the antenna is not in use.

The top plates corresponding to the central chamber and extended channel are mounted directly above the matching bottom plates. Alignment is achieved using aluminum guide

rods that project vertically from various positions on the bottom plates. The guide rods are placed outside of the region of microwave power, usually surrounded by microwave absorber. The planar waveguide spacing is set by several 0.4 in. high cylindrical Teflon spacers, which have only a modest microwave scattering cross section. The scattering from the spacers is detectable, but their effect can be removed by normalizing the final data.

The upper plate of the extended channel is lowered onto the guide rods and allowed to rest on the spacers. The semi-circular upper central chamber plate is connected to a hinged block on the flat side, in which are drilled several through holes. The hinged block is used to align the upper chamber plate, sliding onto corresponding guide rods on a similar block attached to the back of the bottom plate. Once the top plate is in place, it can be rotated upwards (opened) via the hinge mechanism at the back of the plate, allowing access to the inside of the scattering chamber. We have used common hardware store piano hinges on the upper plate; however, we have found that there is some degree of flex and slip in these hinges that limits the reproducibility of the plate positioning and necessitates a correction during analysis for reproducible data. A higher quality hinge might have less play and provide for a more accurate repositioning.

The microwave absorber material, which is sold in large sheets of approximately 0.4 in. thickness, is used in two contexts within the chamber. In the guide region, the absorber is cut into straight sections and used to line the sides of the extended channel. The intent here is that the absorber guide the expanding microwave beam to the aperture, while minimizing reflections back into the guide region. This configuration is more favorable than using conducting walls, which would force the fields to zero at the wall surfaces, resulting in a less uniform front at the aperture. Note that cutting a toothed pattern into the absorber could further minimize reflections, but this would reduce the signal by a greater factor.

Within the central chamber, the purpose of the absorber is to remove all reflections from the periphery of the chamber back into the sample region. By cutting the absorber such that the teeth are at least two wavelengths ( $\sim 3$  cm) long and less than one wavelength between teeth, the absorber should attenuate the reflected signal by 30–50 dB. The apparatus source and detector are coax-to-waveguide couplers (HP X281A), mounted such that the adapter is aligned with the gap between the plates. The X-band waveguide adapter ports have dimensions of 0.4 in. by 0.9 in., giving them a cutoff frequency of 6.56 GHz, and a working frequency range of 8.2–12.4 GHz. The limitation on the high-frequency side is related to higher order mode excitation. Given the 0.4 in. spacing of the plates, 14.8 GHz is the cutoff frequency for the next order propagating mode in the chamber. The potential for higher mode excitation makes operation of the chamber above the X-band frequency range unreliable, as the coupling to the fundamental versus higher order modes depends on the characteristics of the source. Nevertheless, by careful comparison with theoretically predicted scattering curves, we have found empirically that we are able in certain situations to obtain meaningful data up to  $\sim 16$  GHz, although this is not the typical mode used.

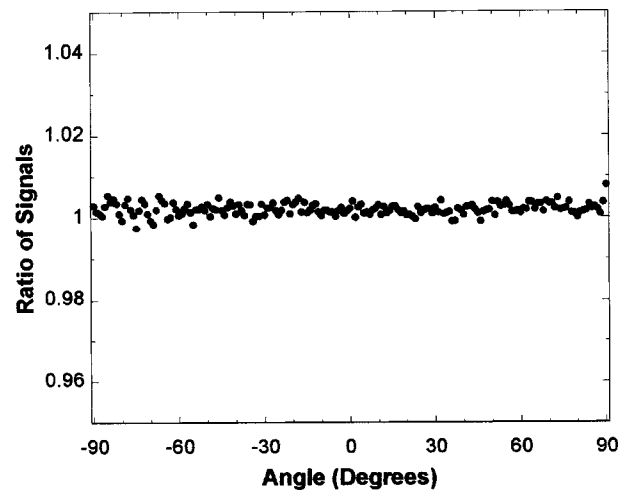


FIG. 5. Experimental data which display the reproducible, low noise angular scan of the ARMS apparatus with the center antenna source radiating without a sample backplane (mode 2). The low noise ratio of two consecutive scans, suggests that by normalizing the instrument to an empty scan, the radiation pattern from a sample backplane can be accurately measured.

In mode 2, an antenna source, which in our case is the projecting pin of a coaxial panel jack receptacle (Applied Engineering Products, model 9004-x113-000 or similar) is used to produce cylindrical waves. In keeping with the two-dimensional confined nature of the ARMS apparatus, we would ideally like to use a linear current source as the localized excitation, which would couple strictly to the lowest propagating modes in the chamber. In reality, our source protrudes into the chamber a finite distance, and produces image charges on the upper and lower plates. The resulting electromagnetic source presumably couples in a complicated manner to the higher order modes of the chamber, although none of these higher order modes propagate at frequencies below 14.8 GHz.<sup>21</sup> Nevertheless, the antenna excitation we use has excellent reproducibility, and can be used to probe antenna/metamaterial interactions.

Figure 5 shows the reproducibility of an angular scan, with the power introduced by the antenna excitation. Two scans were made, and the intensity from one scan divided by the intensity of the second scan. The reproducibility, as determined from the scatter in the measurement, corresponds to  $\sim 30$  dB. For antenna backplane measurements, where  $\sim 0.1$  dB accuracy is typically needed, the ARMS chamber can provide extremely sensitive measurements.

When the ARMS apparatus is used in mode 1, microwaves are introduced in the extended channel where they form a roughly planar beam that strikes an aperture formed from microwave absorber. The beam then undergoes diffraction, leading to the angular intensity distribution shown in Fig. 6 (circle data points). To obtain the data in Fig. 6, the detector is scanned around the circumference of the semi-circular central chamber. The angular resolution of the ARMS is dependent on several factors, including the step size of the motor, the size of the detector, and the diffraction-limited width of the angular intensity distribution. The stepper motor/driver combination has 2404 full steps (4808 half steps) over the  $180^\circ$  range, allowing accurate positioning to better than a tenth of a degree. The X-band detector has a

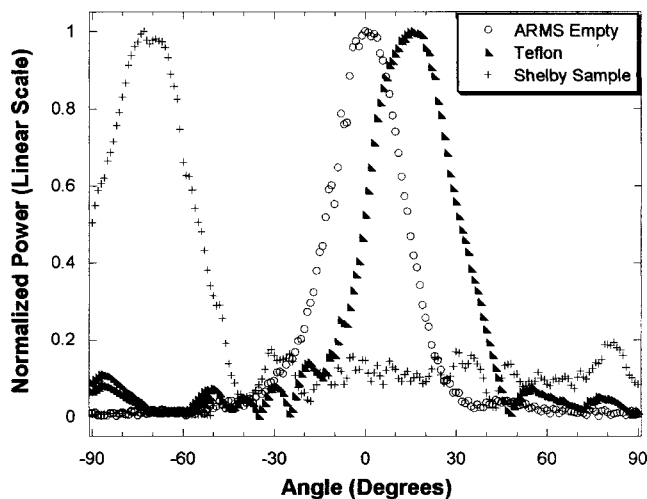


FIG. 6. Experimental data which display the angular resolved refracted ( $16.5^\circ$ ) microwave signal (11.63 GHz) from a plane wave incident (mode 1) on a Teflon wedge ( $n=1.4$ , angle= $32.9^\circ$ ), the refracted ( $-70^\circ$ ) microwave signal on a NIM wedge ( $n=-2.5$  angle= $18.4^\circ$ ), and the unrefracted signal from the same apparatus configuration without a sample present.

port width that subtends approximately  $3.2^\circ$  at the central chamber edge, which sets a limitation on the ARMS resolution. Finally, the width at half maximum of the diffraction curve is roughly  $30^\circ$ , which also implies an ultimate limitation on the angular resolution of measurements made using mode 1, although this restriction can be tuned by changing the characteristics of the aperture. As well, the absolute position of a peak can be determined to a much better precision than the diffraction width.

Examples of refraction data taken on a positive index wedge (Teflon) and a negative index metamaterial (NIM) wedge are also presented in Fig. 6. The metamaterial used for this data is identical to the sample used in Ref. 6 ( $18.4^\circ$  wedge at 11.63 GHz). Clearly, the ARMS apparatus is sufficiently sensitive to detect these refracted signals from our experimental samples

The apparatus is connected to the Agilent vector network analyzer (model 8722ES) via semirigid cable, to the immobile source antenna and waveguide coupler, and via flexible cable (Micro-Coax, UFA210B), to the mobile waveguide coupler detector on the sweeping arm of the apparatus. The semirigid cables have less loss than the flexible cables ( $\sim 5$ – $10$  dB), but the flexible cable is necessary to allow unobstructed movement of the detector. The coaxial cables are not designed to tolerate twisting. Therefore, the angular scanning action must be accompanied by a compliant bend in the attached cable rather than a twist about its axis. We found two ways of connecting flexible cables to the receiver that

minimized twist. The first way is to run the cable along the length of the arm from the rear to the receiver. The second way is to coil the flexible cable in a large loop above the central chamber in such a way that the angular motion of the receiver caused the cable to coil and uncoil.

### III. CONCLUSION

In conclusion, the ARMS apparatus provides highly reproducible automated data acquisition of microwave refraction from positive and negative refracting samples. The flexibility of the instrument allows many types of metamaterial experiments to be carried out efficiently. The two-dimensional character of the measurement allows for easy and cost-effective sample preparation.

### ACKNOWLEDGMENTS

This work is supported by AFOSR (Contract No. F49620-01-1-0440) and DARPA/ONR through a MURI program (Contract No. N00014-01-1-0803).

- <sup>1</sup>D. R. Smith, W. Padilla, D. C. Vier, S. C. Nemat-Nasser, and S. Schultz, *Phys. Rev. Lett.* **84**, 4184 (2000).
- <sup>2</sup>I. V. Lindell, S. A. Tretyakov, K. I. Nikoskinen, and S. Ilvonen, *Microwave Opt. Technol. Lett.* **31**, 129 (2001).
- <sup>3</sup>R. W. Ziolkowski and E. Heyman, *Phys. Rev. E* **64**, 056 625 (2001).
- <sup>4</sup>R. Marques, J. Martel, F. Mesa, and F. Medina, *Phys. Rev. Lett.* **89**, 183 901 (2002).
- <sup>5</sup>V. G. Veselago, *Sov. Phys. Usp.* **10**, 509 (1968).
- <sup>6</sup>R. A. Shelby, D. R. Smith, and S. Schultz, *Science* **292**, 79 (2001).
- <sup>7</sup>C. G. Parazzoli, R. B. Greegor, K. Li, B. E. C. Koltenbah, and M. Tanielian, *Phys. Rev. Lett.* **90**, 107 401 (2003).prl
- <sup>8</sup>A. A. Houck, J. B. Brock, and I. L. Chuang, *Phys. Rev. Lett.* **90**, 137 401 (2003).
- <sup>9</sup>J. B. Pendry, A. J. Holden, W. J. Stewart, and I. Youngs, *Phys. Rev. Lett.* **76**, 4773 (1996).
- <sup>10</sup>J. B. Pendry, A. J. Holden, D. J. Robbins, and W. J. Stewart, *J. Phys.: Condens. Matter* **10**, 4785 (1998).
- <sup>11</sup>J. B. Pendry, A. J. Holden, D. J. Robbins, and W. J. Stewart, *IEEE Trans. Microwave Theory Tech.* **47**, 2075 (1999).
- <sup>12</sup>D. R. Smith, S. Schultz, P. Markos, and C. M. Soukoulis, *Phys. Rev. B* **65**, 195 104 (2002).
- <sup>13</sup>F.-R. Yang, K.-P. Ma, Y. Qian, and T. Itoh, *IEEE Trans. Microwave Theory Tech.* **47**, 1509 (1999).
- <sup>14</sup>D. Sievenpiper, L. Zhang, R. F. Jimenez Broas, N. G. Alexopolous, and E. Yablonovitch, *IEEE Trans. Microwave Theory Tech.* **47**, 2059 (1999).
- <sup>15</sup>R. C. Hansen, *IEEE Antennas Wireless Propagation Lett.* **1**, 46 (2002).
- <sup>16</sup>R. V. Row, *J. Appl. Phys.* **24**, 1448 (1953).
- <sup>17</sup>C. C.-H. Tang, *J. Appl. Phys.* **28**, 628 (1957).
- <sup>18</sup>R. D. Kodis, *J. Appl. Phys.* **23**, 249 (1952).
- <sup>19</sup>R. Marques, F. Medina, and R. Rafii-El-Idrissi, *Phys. Rev. B* **65**, 144 440 (2002).
- <sup>20</sup>C. A. Balanis, *Antenna Theory: Analysis and Design*, 2nd ed. (Wiley, New York, 1997), p. 149.
- <sup>21</sup>T. Suzuki, P. Yu, D. R. Smith, and S. Schultz, *J. Appl. Phys.* **79**, 582 (1996).